science, engineering and health studies

Research Article

Science, Engineering and Health Studies
https://lio1.tci-thaijo.org/index.php/sehs
ISSN (Online): 2630-0087

Application of response surface methodology for optimization of phosphate and ammonia removal from domestic wastewater by modified steel slag

Bui Thi Uyen Uyen[1,2], Dinh Kim Ngan[1,2], Nguyen Nhat Huy[2,3], Nguyen Thi Hoang Hai[1,2], Nguyen Hai Trieu[2,3], and Nguyen Thi Thuy[1,2*]*

[1] School of Chemical and Environmental Engineering, International University, Ho Chi Minh City 700000, Vietnam
[2] Vietnam National University Ho Chi Minh City, Ho Chi Minh City 700000, Vietnam
[3] Faculty of Environment and Natural Resources, Ho Chi Minh City University of Technology, Ho Chi Minh City 700000, Vietnam

***Corresponding author**:
Nguyen Nhat Huy
Nguyen Thi Thuy
nnhuy@hcmut.edu.vn
ntthuy@hcmiu.edu.vn

***Received:** 24 March 2023*
***Revised:** 21 November 2023*
***Accepted:** 21 March 2024*
***Published:** 13 December 2024*

***Citation**:
Uyen, B. T. U., Ngan, D. K., Huy, N. N., Hai, N. T. H., Trieu, N. H., and Thuy, N. T. (2024). Application of response surface methodology for optimization of phosphate and ammonia removal from domestic wastewater by modified steel slag. Science, Engineering and Health Studies, 18, 24020009.

ABSTRACT

Domestic wastewater is one of the significant sources causing phosphorus and nitrogen pollution in natural water. Though steel slags have been applied for the adsorption of phosphate, ammonia, and both in various synthetic and real wastewaters, no report has been found for the application of response surface methodology (RSM) to investigate the main and interaction effects, and optimization of various factors on phosphate and ammonia adsorption by steel slag. The current study aims to evaluate the removal of phosphate and ammonia from domestic wastewater using adsorbents of modified steel slags. Steel slags from two companies were modified, characterized, and preliminarily applied for synthetic wastewater treatment to select the suitable type of steel slag. Optimization experiments were then designed using RSM to find the significant factors, their interactions affecting the treatment processes, and optimum conditions. The results of energy-dispersive X-ray spectroscopy (EDS) and Brunauer–Emmett–Teller (BET) analyses showed that thermal treatment affected the mass percentages of elements and increased the surface areas of the materials. The adsorption kinetics and isotherm studies demonstrated that the phosphate adsorption process followed pseudo-second-order reaction kinetics, and the Langmuir model was appropriate to the present experimental results. The results from RSM suggested that output phosphate concentration was significantly affected by the modified temperature, steel slag dosage, contact time, and the modified temperature-dosage interaction, while the modified temperature and steel slag dosage were significant factors for output ammonia concentration. Validation of the domestic wastewater treatment at the optimum conditions including the modified steel slags at 776°C, contacting time of 15.7 h, and dosage of 0.87 g/L confirmed the high removal efficiency for phosphate (81.7%), while ammonia and COD were eliminated at the efficiencies of 31.6% and 32.7%, respectively. This study hence proposed the application of the modified steel slag as a promising and cheap adsorbent for nutrient removal in domestic wastewater.

Keywords: modified steel slag; ammonia removal; phosphate removal; response surface methodology; domestic wastewater

1. INTRODUCTION

Excessive amounts of phosphate and ammonia may cause eutrophication and algal blooms that lessen the functions and services of aquatic ecosystems (Ambulkar, 2017; Lim et al., 2018). Eutrophication is a serious consequence of the fertility of these nutrients in wastewater, especially domestic sewage discharged into water bodies (Preisner et al., 2020; Song et al., 2011). In addition, the amounts of phosphate and ammonia in water are the controlling factors for algal growth, which possibly causes algal blooms. Based on the proportional contributions from individual sources, Mockler et al. (2017) concluded that one of the main sources of phosphate is municipal wastewater treatment plants. Due to their severe impact on the environment, the governments in some countries decided to promulgate discharge regulations for limiting the concentrations of phosphorus and nitrogen in wastewater, especially Vietnam's technical regulation on domestic wastewater, QCVN 14:2008/BTNMT (5 mg/L for ammonium and 6 mg/L for phosphate) (MONRE, 2008).

Technologies have been proposed extensively for the removal of phosphate and ammonia in wastewater over the past century. Previous researchers have demonstrated that nutrients can be eliminated by physicochemical methods including oxidation (Garrido-Cardenas et al., 2020), coagulation-flocculation and precipitation processes (e.g., with aluminum Al(III), Fe(III) (Garrido-Cardenas et al., 2020). Lime $Ca(OH)_2$ (Dunets and Zheng, 2014) and NaOH (Yan et al., 2014)), adsorption by activated carbon residue from biomass gasification (Kilpimaa et al., 2015), biological removal using moving bed biofilm reactor (Kermani et al., 2009), as well as physical methods with membrane separation (Luo et al., 2017) and nanofiltration (Zhao et al., 2021) have also been used. Among these methods, adsorption is one of the crucial processes for removing phosphorus from aqueous solutions due to its great loading capacity and strong affinity with the advantages of high treatment effectiveness, without the formation of precipitates, flexibility, and convenience of use (Jafari and Moslemzadeh, 2022). This is especially true when adsorbents are inexpensive and widely accessible (Abd El-Azim et al., 2019).

Various low-cost adsorbents have been tested in several studies such as fly ash, bituminous coal, coconut shell, mango seed and shell, bagasse, used waste tea leaves, wood barks, red mud, blast furnace slag, and steel slag (Abd El-Azim et al., 2019; Ji et al., 2022). Among them, steel slag is an industrial byproduct generated in a large amount from the steel manufacturing industry. The steel slag has a wide range of uses for recovery and recycling such as in aggregates of reinforced concrete constructions, road building, and hydraulic structures. With its high surface area, porous structure, high mechanical strength, and abundant metal oxides such as Fe_2O_3, Al_2O_3, and CaO, steel slag has a strong adsorption capacity and high ion-exchange ability, leading to its potential application in wastewater treatment (Abd El-Azim et al., 2019; Ji et al., 2022; Jafari and Moslemzadeh, 2022). Obviously, utilizing steel slag to treat wastewater is not only for using waste to treat other wastes but also to decrease the stock of metallurgical slag (Ji et al., 2022). Ji et al. (2022) stated that metallurgical slag contained Pb, Zn, As, Cr, Mn, and other heavy metals, and that utilizing it directly without treatment would contaminate the environment, but Gwon et al. (2018) and Shi et al. (2022) confirmed that the toxic heavy metals in the leachate of steel slag were either not detected or did not exceed the maximum limit values regulated in the surface water standard. In addition, none of the slags exceeded U.S. EPA standards used for evaluating slag as an environmentally hazardous material (Gwon et al., 2018; Shi et al., 2022).

Currently, steel slag is considered a potential and efficient material for the removal of phosphorus from wastewater (Jafari and Moslemzadeh, 2022) due to its wide availability, sufficient ionic concentrations for utilization in the process, and strong adsorption capability (T. Park et al., 2017). There are many studies focused on the applications of steel slag and its modification for phosphate treatment from synthesis wastewater (Ahmad et al., 2020; Barca, 2014; Bowden et al., 2009; Liu et al., 2022; J.-H. Park et al., 2017; Roychand et al., 2020; Xue et al., 2009), real wastewater such as wastewater discharged from hydroponic cultivation (J.-H. Park et al., 2017), municipal wastewater (Pramanik et al., 2020; Qiu et al., 2022), and agricultural tile drain effluent (Steinman et al., 2022). Steel slags have also been applied for ammonia removal in synthetic wastewater (Dhoble and Ahmed, 2018), and ammonia nitrogen and total Kjeldhal nitrogen from domestic wastewater (Hamdan et al., 2021). In addition, several studies aimed to remove both phosphate and nitrate in synthetic wastewater (Hua, 2016), and phosphate and ammonia in synthetic wastewater (Jha et al., 2008; Ping et al., 2016) and in domestic wastewater (Wang et al., 2021). Though steel slag has been applied for the adsorption of phosphate, ammonia, and both in various synthetic and real wastewaters, most studies above use the "one-factor-at-a-time" approach for their experimental design to investigate the effect of various factors on the treatment process. To the best of our knowledge, there is no study using response surface methodology (RSM) for the investigation and optimization of the phosphate and ammonia adsorption process by steel slag. Therefore, this study was conducted to evaluate the effectiveness of ammonia and phosphate removal from domestic wastewater by basic oxygen furnace (BOF) modified steel slags. Preliminary experiments were conducted to select the type of steel slags, and their kinetics and isotherms were studied. In the next step, adsorption experiments were designed using RSM, which allowed evaluating factors and their interactions affecting phosphate and ammonia removal, suggesting optimum working conditions for both dependent responses as phosphate and ammonia removals. In the final step, validation of the optimal conditions was conducted using actual domestic wastewater.

2. MATERIALS AND METHODS

2.1 Domestic wastewater sampling and preparation of synthetic wastewater

2.1.1 Domestic wastewater sampling

Samples were collected from the equalization tank of a Vietnam National University–Ho Chi Minh City (VNU-HCM) dormitory wastewater treatment plant on different days using 2-L bottles. The ammonia, phosphate, and COD concentrations in these samples were measured immediately after sampling. All measurements were repeated three times and the average values with their standard deviations are presented in Table 1.

Table 1. VNU-HCM — dormitory's domestic wastewater characteristics

Sampling date	pH	Input phosphate concentration (mgPO_4^{3-}/L)	Input ammonia concentration (mgNH_3^-N/L)	Input COD (mg/L COD)
01/03/2022	-	8.72±0.13	28.0±0.1	-
02/03/2022	-	8.37±0.00	-	-
03/03/2022	-	9.60±0.24	42.0±0.3	-
14/06/2022	-	9.24±0.31	33.6±0.2	124.8±6.6
24/06/2022	6.92	-	-	-
07/02/2023	6.87	7.77±0.48	36.2±2.0	125.0±10.3
20/02/2023	7.10	8.65±0.28	45.5±1.5	188.2±6.8
Average	6.96±0.12	8.76±0.60	36.6±6.3	146.0±26.5

2.1.2 Synthetic wastewater sample

The phosphate and ammonia concentrations in synthetic wastewater samples were set based on the real concentrations of these parameters collected from the domestic wastewater source previously mentioned. Accordingly, phosphate and ammonia at the concentrations of 10 mg PO_4^{3-}/L and 42 mg NH_3^-N/L were prepared by dissolving KH_2PO_4 and $(NH_4)_2SO_4$, respectively, in distilled water.

2.2 Absorbent preparation and adsorption experimental design

2.2.1 Collection and modification of steel slag

Adsorbents were made of the BOF steel slags taken from Da Nang Steel Joint Stock Company (DN), and Green Materials Co., Ltd from Ba Ria–Vung Tau (GM). The steel slags were modified following a procedure given in Figure S1 (Supplementary Data). Steel slag was collected through a sieve mesh with a size of 0.45 mm, and heated at 364, 500, 700, 800, 900, and 1036°C. The images of the raw and modified DN and GM steel slags at various temperatures can be found in Figure S2 (Supplementary Data). The adsorbent materials were stored in a dehumidifier. The surface morphology of the steel slags was then characterized by scanning electron microscopy (SEM), energy-dispersive X-ray spectroscopy (EDS) (JOEL, JSM-IT200), and X-ray diffraction spectroscopy (XRD, Model D2 Phaser, Bruker). The surface area and porous structure of the steel slags were determined using the BET (Brunauer–Emmett–Teller) (Model Surfer, Thermo Scientific).

2.2.2 General adsorption procedure

Specific amounts of steel slag were added to flasks containing 50 mL of wastewater. At room temperature, the flasks were shaken at 150 rpm in a thermostatic rotary shaker. Depending on the purpose of the test, the number of variables (e.g., calcination temperature of the material, material dosage, and contact time) and their values were varied. Before and after treatment, the concentrations of pollutants were measured. Each experiment was repeated three times.

2.2.3 Preliminary experiments

Raw DN and GM steel slags and their modified material heated at 500 and 900°C were used in preliminary experiments to identify their ability to adsorb ammonia and phosphate in synthetic wastewater. The adsorption process was conducted with the adsorbent dosage of 0.8 g/L, contact times of 2 and 24 h, and at pH 6. Solutions at the initial concentrations of either 10 mg PO_4^{3-}/L or 42 mg NH_3^-N/L ammonia were prepared.

To study the kinetics of the phosphate adsorption process, the phosphate solution (initial concentration of 10 mg/L, pH 6) was treated with 1.2 g/L of modified steel slag (heated at 800°C) at various contact times (0–24 h). After each contact time, the samples were taken for phosphate measurement. The experimental data were then fit to pseudo-first-order (Equation 1), pseudo-second-order kinetic (Equation 2), intra-particle diffusion (Equation 3), and Elovich (Equation 4) models.

$$\ln(q_e - q_t) = \ln q_e - k_1 t \quad (1)$$

$$\frac{t}{q_t} = \frac{1}{(k_1 q_e^2)} + \frac{t}{q_e} \quad (2)$$

$$q_t = k_p t^{\frac{1}{2}} + C \quad (3)$$

$$q_t = \left(\frac{1}{\beta}\right) \ln(\alpha\beta) + \left(\frac{1}{\beta}\right) \ln t \quad (4)$$

where k_1 and k_2 are the first-order and second-order apparent adsorption rate constants (min^{-1}); k_p is the intra-particle diffusion rate constant ($mg/g/min^{\frac{1}{2}}$); C is the thickness of the boundary layer; q_t and q_e are the amounts of pollutant adsorbed (mg/g) at time t (min) and at equilibrium, respectively; α (mg/g/min) is the initial rate of adsorption and β is the adsorption constant.

The adsorption isotherms were studied with different pollutant concentrations (5–200 mg/L) at pH 6 using the adsorbent of 1.2 g/L for 5 h. The data were fitted to Langmuir (Equation 5) and Freundlich (Equation 6) models (Mahmoodi and Maghsoodi, 2015).

$$\frac{1}{q_e} = \frac{1}{q_m} + \frac{1}{K_L \times q_m \times C_e} \quad (5)$$

$$\log q_e = \log(K) + \frac{1}{n} \log C_e \quad (6)$$

where q_m (mg/g) is the maximum adsorption capacity per monolayer of adsorbent; K_L (L/mg) is the Langmuir constant; C_e (mg/L) is the absorbent concentration at equilibrium; K_F (mg/g) is Freundlich constant; and 1/n is the adsorption intensity.

2.2.4 Optimization process using response surface method—central composite design and validation

The output phosphate and ammonia concentrations were the dependent variables whereas the modified temperature, adsorbent dosage, and contact time were the independent variables, as listed in Table 2.

Table 2. Three factors at various levels for central composite design

Factors	Levels				
	Low (–1)	(0)	High (+1)	– alpha	+ alpha
A - Temperature modification (°C)	500	700	900	363.6	1036.4
B - Steel slag dosage (g/L)	0.4	0.8	1.2	0.1272	1.4728
C - Contacting time (h)	6.5	15.3	24	0.5326	29.9675

The central composite design (CCD) is a two-level factorial design with center, factorial, and axial points. The number of experiments in a central composite design is determined by Equation 7 when the factorial design is full.

$$N = 2^K + 2k + N_0 \quad (7)$$

where k is the number of independent variables (factors), 2^K is the number of factorial points, and 2k is the number of star points. The levels of the points on a star design are ±α where |α|≥1; N_0 is the number of center points.

In this study, there were three factors, leading to 6 center points (α = 1.682), 24 factorial points (i.e. 2^3 with 3 replicates for each), and 18 axial points (i.e. 2×3 with 3 replicates for each). Hence, there were a total of 48 experiments as presented in Table 7. Based on the experimental data, the outcome of the response surface regression (Y) is the following mathematical paradigm - quadratic surface model shown in Equation 8 (Sibiya et al., 2022)

$$Y = \beta_0 + \beta_1 A + \beta_2 B + \beta_3 C + \beta_{12} AB + \beta_{13} AC + \beta_{23} BC + \beta_{11} A2 + \beta_{22} B2 + \beta_{33} C2 \quad (8)$$

where Y is the predicted response; A, B, and C are the coded independent variables; β_0 is the mean value of the response constant coefficient; β_1, β_2, and β_3 are linear coefficients; β_{11}, β_{22}, and β_{33} are quadratic coefficients; and β_{12}, β_{13}, and β_{23} are interaction coefficients.

The Design Expert software was employed for statistical regression and graphical analyses of the obtained data. Adsorption experiments were then conducted using 250-mL Erlenmeyer flasks containing 50 mL of the synthetic wastewater with initial concentrations of 10 mg PO_4^{3-}/L and 42 mg NH_3^-N/L at pH 6.

Validation of optimization conditions for domestic wastewater was then performed. The optimal conditions found in the optimization experiments were applied for real domestic wastewater taken on 14 June 2022, 7 and 20 February 2023.

2.3 Analytical method and data analysis

The phosphate concentrations were measured by the 930 Compact IC Flex Ion Chromatograph (Metrohm AG, Switzerland). Ammonia concentrations were analyzed following two processes, including distillation (4500-NH3 B) using Pro Nitro-S equipment (JPSELECTA, Spain) and titration with hydrochloric acid (4500-NH3 C) (APHA et al., 2005). COD was determined according to the closed reflux method (5220) (APHA et al., 2005). After data collection, the removal efficiency and adsorption capacity of phosphate, ammonia, and COD were determined by Equation 9 and Equation 10 (Mokhtari-Shourijeh et al., 2020).

$$E(\%) = \frac{C_o - C_e}{C_o} \times 100 \quad (9)$$

$$q_e = \frac{C_o - C_e}{m} \times V \quad (10)$$

where E(%) is the pollutant removal efficiency, q_e is the adsorption capacity at equilibrium in milligrams of pollutant per gram of adsorbent, C_o (mg/L) is the initial pollutant concentration, C_e (mg/L) is the equilibrium concentration of pollutant remaining in the solution, V (L) is the sample volume, and m (g) is the mass of the adsorbent.

3. RESULTS AND DISCUSSION

3.1 Material characterization

Figure 1 illustrates the SEM images of the raw and modified DN steel slags at different temperatures. Obviously, the DN raw and modified steel slags had irregular shapes and sizes. From EDS analysis, the elemental mapping of DN raw and modified steel slags is given in Supplementary Data. Table 3 shows the components of DN raw steel slags (X-0) and modified steel slags at 700, 800, and 900°C (denoted as X-700, X-800, and X-900, respectively), and X-F (modified steel slag at 800°C, after phosphate adsorption). When the calcination temperature increased, the element contributions reduced from 10.03 to 3.93% for C and from 53.13 to 37.06% for O. These reductions would be due to the burning of these elements being stronger at higher temperatures. The mass contribution of Ca was from 34.48 to 55.48%, which is consistent with the results from Kim et al. (2006) (40.5%), J.-H. Park et al. (2017) (49.8%), and Xue et al. (2009) (45.4%). This element at a high level would be very important for the treatment of phosphate and ammonia as the principal removal mechanisms were the formation of calcium phosphate precipitation (Ping et al., 2016), and ion exchange with Ca^{2+} (Wang et al., 2021), respectively. The mass percentages of other elements such as Mg, Si, and Al were 0.00–1.02, 1.57–3.22, and 0.00–0.43%, respectively, which were smaller compared to the aforementioned elements.

The results of the BET analysis of the absorbent calcined at 800°C (X-800) and 700°C (X-700) are shown in Figure 2(a) and 2(b), respectively. The pore volume and specific surface area of X-800 were 1.69 cm^3/g and 7.35 m^2/g, respectively, which were higher than those of X-700 (1.47 cm^3/g and 6.38 m^2/g, respectively). In comparison with previous studies, the surface areas of adsorbent in our study were larger than those of Trang et al. (2018) (0.32 m^2/g), Xue et al. (2009) (0.9 m^2/g), Kim et al. (2006) (930 cm^2/g), Trinh et al. (2022) (1.9 m^2/g for raw steel slag, 2.5 m^2/g after NaOH modification), Trinh et al. (2023) (0.09 m^2/g for raw steel slag, 2.3 m^2/g after the acidic activation), Gao et al. (2017) (3.46 m^2/g), but slightly lower than those from Yu et al. (2015). In his study, the

surface area of raw steel slag was 7.523 m^2/g, increasing to 8.62 m^2/g after modification at 800°C for 1 h. The trend of increasing surface area due to the increased temperature is consistent with the findings from Yu et al. (2015) and Yang et al. (2017). According to Yang et al. (2017), a high modification temperature can remove some contaminants and water molecules and open channels inside and outside the steel slag, thereby increasing the pore size and creating a high pore density. His research found that the modification of steel slags at 800°C resulted in an increase in the specific surface area of 3.34 times that of the original form.

Table 3. The elemental component of raw and modified DN steel slags

Element	Mass (%)			
	X-0	X-700	X-800	X-900
C	10.03±0.04	9.56±0.03	5.03±0.03	3.98±0.02
O	53.13±0.17	49.98±0.17	46.62±0.17	37.06±0.17
Mg	0.74±0.02	0.83±0.02	1.02±0.03	-
Al	-	0.18±0.02	0.43±0.02	0.27±0.02
Si	2.62±0.04	1.57±0.03	2.52±0.04	3.22±0.05
Ca	34.48±0.22	38.37±0.23	44.37±0.25	55.48±0.29
Total	100	100	100	100

As can be seen in Figure 2(c), the XRD results of the raw material show that the peaks were mainly $CaCO_3$ at 2θ = 18.18° and 29.48° corresponding to crystal planes (101) and (112) (Li et al., 2018). After being calcined at 700°C, this component gradually decreased, probably due to the partial pyrolysis of $CaCO_3$ into CaO. At a temperature of 800°C, the pyrolysis of $CaCO_3$ took place completely and the CaO peaks appeared at 2θ = 32.25°, 33.55°, 37.43°, 43.04°, 46.81°, and 53.94°, corresponding to the planes of (040), (200), (002), (015), (204), and (222), respectively. There was also the appearance of other metal oxides such as Mg, Si, and Al at 2θ = 43.04° corresponding to the (015) plane (Fang et al., 2018; Xue et al., 2009). These elements were also found in the EDS elemental mapping of the materials (Table 3). After phosphate adsorption onto steel slag, a significant change of the peaks was observed from 10 to 80°, indicating that the phosphate adsorbed on steel slag changed the intensity of the component peaks (X-F line in Figure 2(c)). Consistent with previous research results, there was contact between phosphate salts (Al, Ca, Fe) at 2θ = 37.43° and 33.55°, corresponding to planes (002) and (200) and slag particles (Oguz, 2004). After phosphate adsorption, the maximum intensity of some peaks at 2θ = 37.43° and 33.55° decreased, which could be attributed to the hydrolysis of $Ca_2Fe_2O_5$, Ca_2SiO_4, $Ca_{14}Mg_2(SiO_4)_8$ $CaFe_2O_4$, CaO and FeO (J.-H. Park et al., 2017).

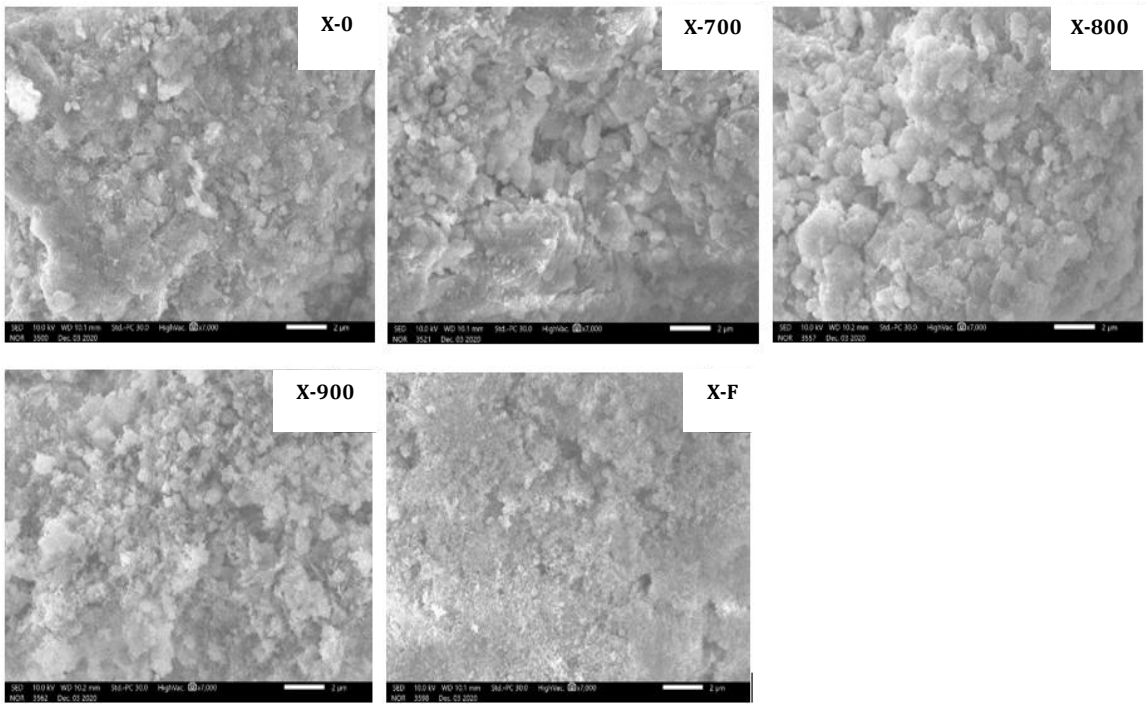

Figure 1. SEM images of raw and modified steel slags

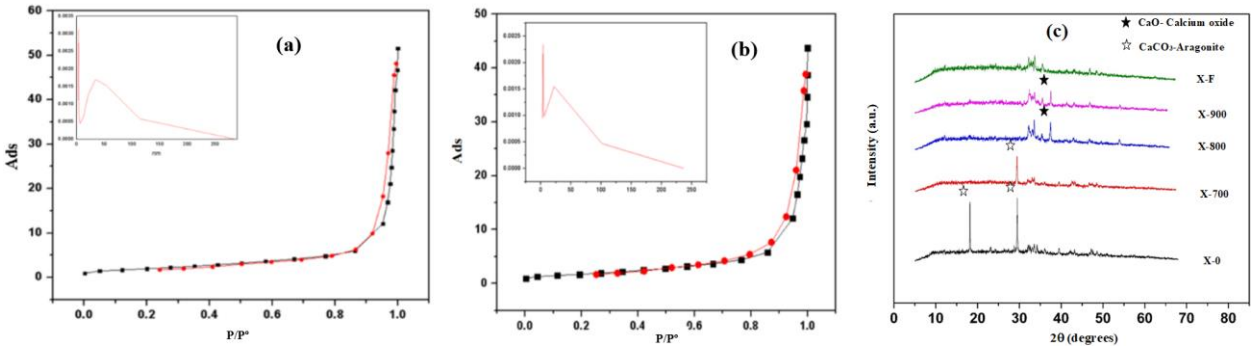

Figure 2. The BET analysis of the absorbents calcined at (a) 800°C, (b) 700°C, and (c) the X-ray diffraction spectrum

3.2 Results of preliminary experiments

3.2.1 Adsorbent selection

These experiments preliminarily evaluated the phosphate and ammonia removal efficiency by two types of raw steel slags and their modified adsorbents to select the material with high removal efficiencies. Figure 3a shows that the raw and modified DN steel slags provided better phosphate removal efficiency than those of GM steel slags, with an exception at 2 h and 900°C. At this exception point, the phosphate removal efficiency of GM was 32.3%, which was higher than that of DN (27.5%). Similarly, the raw and modified DN steel slags also resulted in higher ammonia removal efficiencies than the remaining types of steel slags, with exceptions at 24 h for the raw and the steel slags calcined at 500°C (Figure 3b). In addition, increasing the calcination temperature led to a higher removal efficiency of DN steel slags for both phosphate and ammonia, but depending on the contact time, the effect of temperature was unstable for the adsorption ability of GM steel slags. Also, the contact time seemed to positively affect the removal efficiency of phosphate in which the adsorption for 24 h provided better removal efficiency compared to that for 2 h. However, this factor effect was not clear in the case of using DN steel slags for ammonia removal. To sum up, the modified DN steel slags mainly provided higher treatment efficiency for both phosphate and ammonia, thus they were selected for further experiments. Effects of contact time and calcination temperature on the adsorption ability of the materials were initially assessed, but there was a need for further confirmation as the parameters in these experiments were separately investigated with only two to three levels (e.g., 2 and 24 h for contact time, and 0, 500, and 900°C for calcination temperature) while the interactions between them had not been considered. Hence, experiments were designed following RSM to find the factors' effects and optimization conditions in the next section.

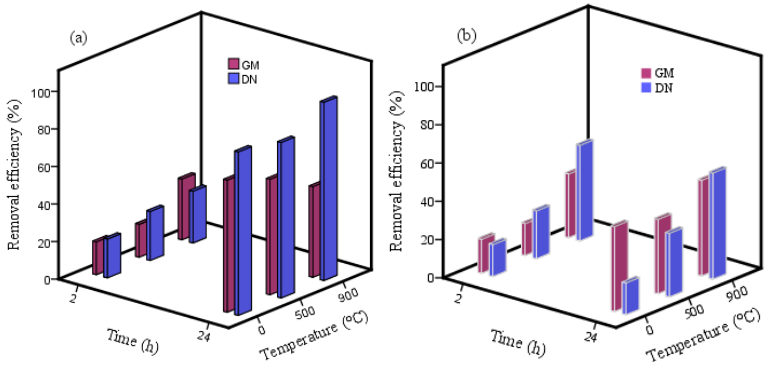

Figure 3. (a) Phosphate and (b) ammonia removal efficiency by different modified steel slags (C_o = 10 mg PO_4^{3-}/L and 42 mg NH_3^-N/L, steel slag dose: 0.8 g/L; contact time: 2 and 24 h)

3.2.2 Adsorption kinetics and isotherms

The time dependence of phosphate adsorption is illustrated in Figure 4a. Phosphate output concentration reduced very fast from 10 mg/L to less than 1 mg/L after 2 h, then slowly, and subsequently reached 0.5 mg/L after 9 h. The trend of time dependence of the phosphate output concentration in this study is consistent with the findings from Liu et al. (2022) who used an electric arc furnace (EAF) slag aggregate for the treatment of a P solution. The adsorption process was fitted to four kinetic models, including pseudo-first-order (PFO), pseudo-second-order (PSO), intra-particle, and Elovich kinetic models with the parameters displayed in Figure 5 and Table 4. It can be noted that the PSO model provided the highest value of the coefficient of determination (R^2) in comparison to the PFO, the intra-particle diffusion, and the Elovich models. Therefore, the PSO kinetic model fitted better with the experimental result of adsorption, indicating the rate-limiting step being chemisorption (Sahoo and Prelot, 2020). This finding is consistent with the kinetic models reported from da Silva et al., (2022) and Kadirova et al., (2015), but not consistent with Han et al. (2015) who found that the removal process of phosphorus through BOF-slag followed PFO reaction kinetics. Based on the PSO

equation, the equilibrium adsorbed capacity was 8.4246 mg/g, which was much greater than those for other models.

Figure 4b shows the relation between the equilibrium concentrations of phosphate in the liquid (C_e) and solid phases (q_e). To describe the adsorption on active sites, the data were fitted to Langmuir and Freundlich models. Figure 6 presents the linear forms of Langmuir and Freundlich models, while the models' parameters were calculated and are shown in Table 5. The R^2 values for Langmuir and Freundlich isotherm models were 0.9905 and 0.6621, respectively, indicating that the Langmuir isotherm was the best for fitting the experimental data. This finding is consistent with that from the literature (da Silva et al., 2022; Wang et al., 2021; Yu et al., 2015), suggesting that the adsorption of phosphate occurred as a monolayer on the homogeneous surface of modified steel slag and each active site of modified steel slag provided the same affinity for adsorbate molecule.

Besides, the maximum adsorption capacity (q_{max}) of phosphate on steel slag from the Langmuir equation was 31.0559 mg PO_4^{3-}/g (i.e., 10.1340 mg P/g). For comparison, the q_{max} values of phosphate on the modified steel slag from previous literature were summarized in Table 6. It is noted that though the studies in Table 6 were intentionally selected due to their initial phosphate concentrations being close to the phosphate concentration in general domestic wastewater, this comparison is for reference only since there were differences in the experimental conditions such as steel slag doses, initial P concentrations' ranges, and contact times. Obviously, modified steel slag provided a relatively higher q_{max} value than those from almost all studies using steel slag for phosphate treatment in the literature

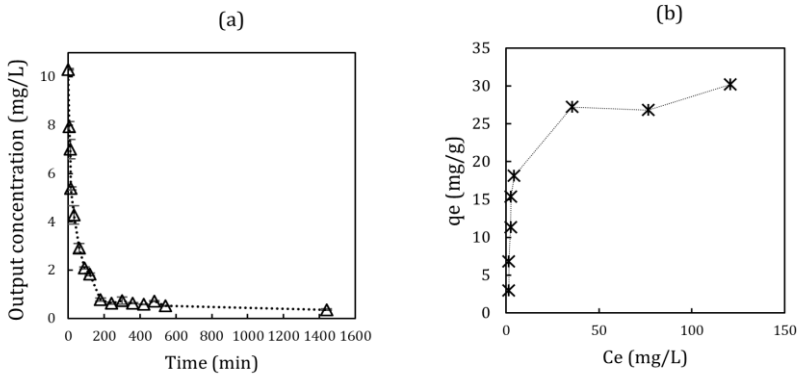

Figure 4. (a) Effect of contact time, and (b) isotherm data of phosphate adsorption on the modified steel slag

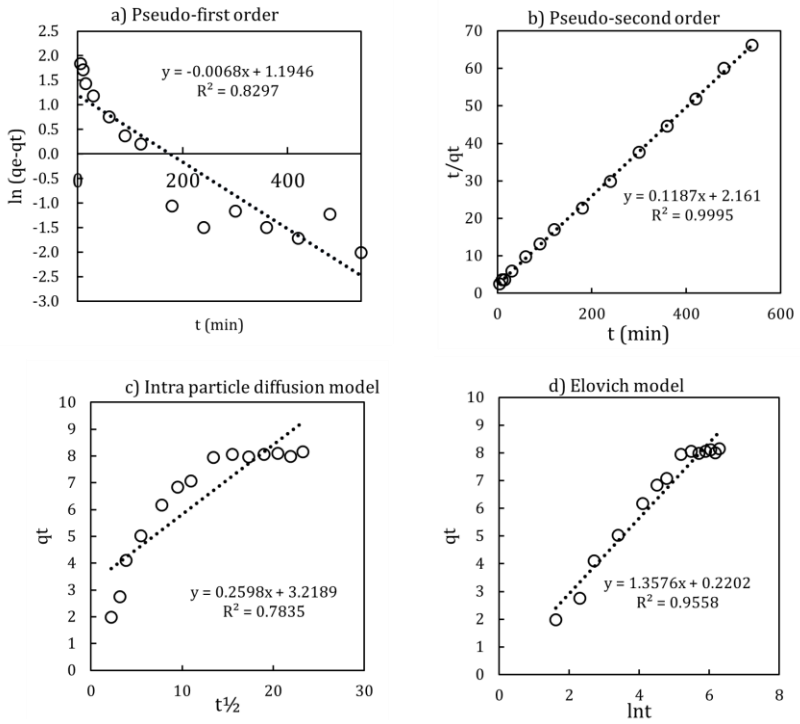

Figure 5. Adsorption kinetics of (a) the pseudo-first-order, (b) pseudo-second-order kinetic, (c) intra-particle diffusion, and (d) Elovich models of phosphate adsorption

Table 4. Kinetic parameters calculated for phosphate adsorption onto modified steel slag

Model	Parameter	Unit	Value
Pseudo-first order (PFO)	k_1	min^{-1}	0.0068
	q_e	mg/g	3.3022
	R^2	-	0.8297
Pseudo-second order (PSO)	k_2	mg/(g.min)	0.0065
	q_e	mg/g	8.4246
	R^2	-	0.9995
Intra-particle diffusion	k_3	$mg/(g.min^{\frac{1}{2}})$	0.2598
	C'	mg/g	3.2189
	R^2	-	0.7835
Elovich	α	mg/(g.min)	646.1064
	β	mg/g	0.7366
	R^2	-	0.9558

Regarding the adsorption mechanisms, previous studies suggested that chemical precipitation and surface complex such as the ligand exchange between phosphate (in solution) and –OH (on the surface of BOF slag) are the main adsorption mechanisms of phosphate on steel slag (Wang et al., 2021; Xue et al., 2009; Yu et al., 2015). The chemical precipitation occurred when Ca^{2+}, Fe^{2+}, and Al^{3+} hydrolyzed from steel slag reacted with phosphates to form Ca-P and other precipitations. The ligand exchange could be described as the reactions in Equation 11 and Equation 12 (Xue et al., 2009).

$$2 \equiv Si - OH + H_2PO_4^- \Leftrightarrow (\equiv Si)_2HPO_4 + H_2O + OH^- \quad (11)$$

$$2 \equiv Al - OH + H_2PO_4^- \Leftrightarrow (\equiv Al)_2HPO_4 + H_2O + OH^- \quad (12)$$

There is a limitation that this study has not investigated the kinetics and isotherms for ammonia adsorption on steel slag. Qiu et al. (2015) studied adsorption kinetics and isotherms of ammonia-nitrogen on steel slag and found that the controlling step of NH_4^+-N adsorption varied under different experimental conditions and the kinetics of adsorption can be described by Boyd's equation, Kannan's equation and the PSO kinetic model. In addition, the isotherm of NH_4^+-N was better fitting on the Langmuir model (Jinming et al., 2012). Ion exchange between the metal ions of the steel slag surface and ammonia, and physical adsorption were the main adsorption mechanisms of ammonia on steel slag (Jinming et al., 2012; Wang et al., 2021).

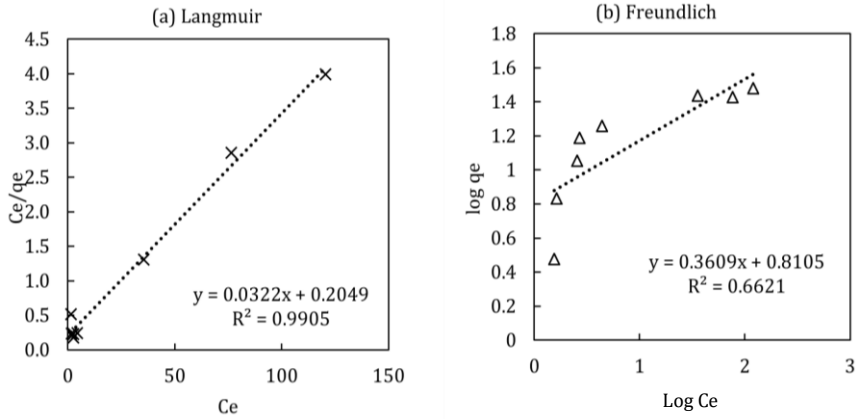

Figure 6. (a) Langmuir and (b) Freundlich models

Table 5. Parameters of isotherm models

Isotherm	Parameter	Value
Langmuir	q_{max}	31.0559
	K_L	0.1571
	R^2	0.9905
Freundlich	K_F	6.9263
	n	2.7709
	R^2	0.6621

Table 6. Comparison of q_{max} values achieved from modified steel slag

No.	Adsorbent	Experimental conditions	Adsorption capacity (q)	References
1	Modified steel slag (Heated at 800°C) (5 g/L)	Synthetic solution 10–125 mgP/L, 24 h	q_{max}: 13.620 mg P/g	Yu et al. (2015)
2	Steel slag (40 g/L)	Synthetic solution: phosphate: 2.5–12.5 mg/L	q_{max}: 1.39 mg PO_4^{3-}/g	Ping et al. (2016)
3	Steelmaking slag (40 g/L)	Synthetic wastewater: 5–100 mg PO_4^{3-}/L, pH 5, 45 min	q_{max}: 3.8 mg PO_4^{3-}/g;	Pramanik et al. (2020)
4	Modified granular steel slag (GSS) (thermal treatment) (10 g/L)	Synthetic solution 24 h	q_{max}: ~7.037 mg PO_4^{3-}/g	Wang et al. (2021)
5	Electric arc furnace (EAF) slag aggregate (10 g/L)	Synthetic solution: 5–50 mg P/L, pH 7	q_{max}: 1.81 mg P/g	Liu et al. (2022)
6	Blast furnace sludge (BFS) (50 g/L)	Synthetic solution:20–200 mg P–PO_4^{3-}/L, pH 6, 24 h	q_{max}: 6.48 mg P/g	da Silva et al. (2022)
7	Modified steel slag (1.2 g/L)	Synthetic solution: 5–200 mg PO_4^{3-}/L, pH 6, 5h	q_{max}: 31.0559 mg PO_4^{3-}/g (10.1340 mg P/g)	This study

3.3 Results of optimization experiments

3.3.1 Experimental results and ANOVA analysis

Previous studies have addressed the effects of calcination temperature (Jha et al., 2008; Yu et al., 2015), pH (Ahmad et al., 2020; Liu et al., 2022; J.-H. Park et al., 2017; Ping et al., 2016; Xue et al., 2009), size of steel slag (Barca, 2014; J.-H. Park et al., 2017), steel slag dosage (J.-H. Park et al., 2017; Ping et al., 2016; Wang et al., 2018), reaction time (Ping et al., 2016), and aeration (Ahmad et al., 2020) on the phosphate treatment by steel slags. Regarding the effect of pH, although Ahmad et al. (2020) found high removal efficiencies of orthophosphate regardless of the pH of the influents, better efficiencies were found at pH 3 and 5 compared to those at pH 11. Similarly, Han et al. (2015) found that apparent rate constant was greatly decreased with increasing initial pH from 3.0 to 7.0. In addition, J.-H. Park et al. (2017) and Pramanik et al. (2020) reported the maximum phosphate adsorption capacities were at pH 5. However, Liu et al. (2022) reported that the P removal capacity of EAF slag increased gradually with the increase of pH from 2 to 10 with the highest P removal capacity of 1.94 mg/g achieved at pH 12. Despite the different findings in pH effects from those studies, it was decided to keep the pH of the treatment at the original pH of domestic wastewater (i.e., of about 6.9, Table 1) for this study. This decision was made because domestic wastewater is typically produced in large quantities, and if pH adjustment is applied prior to the treatment, there would be a high chemical consumption for neutralization before discharging the treated wastewater.

In general, a smaller steel slag size can achieve a higher adsorption efficiency of PO_4^{3-}-P, possibly due to its higher surface area (Barca et al., 2014; Bowden et al., 2009; J.-H. Park et al., 2017; T. Park et al., 2017). The sizes of steel slag varied from different studies such as 10–20 µm (Jha et al., 2008), <300 µm (Bowden et al., 2009), 0.5–6 mm (T. Park et al., 2017), 0.8–2.3 and 2.3–4.6 mm (J.-H. Park et al., 2017), and 6–12 mm and 20–50 mm (Barca et al., 2014). In this study, to reduce the number of factors in the optimization process, a 0.45 mm steel slag was selected, which is considered in the smaller ranges in the comparison with previous studies. Similarly, studies have either stirred the solution at 150 rpm (Ahmad et al., 2020; Bowden et al., 2009), 200 rpm (Wang et al., 2021), or applied shaking at 100 rpm (Hua et al., 2016). Shaking the solution at 150 rpm was therefore selected in this study. Three main factors were considered in the experimental design, including calcination temperature of the adsorbent, steel slag dosage, and contact time while two responses were the output concentrations of ammonia and phosphate. Table 7 shows the outline of 48 tests of optimization experiments and the results of the experiments. The effects of various factors and optimal conditions for achieving the minimum output of phosphate and ammonia concentrations were evaluated.

Table 7. Results for central composite design matrix

Run	A: Temperature modification (°C)	B: Steel slag dosage (g/L)	C: Contacting time (h)	Output ammonia concentration (mg NH_3-N/L)	Output phosphate concentration (mg PO_4^{3-}/L)
1	1036	0.8	15.3	20.9	0.582
2	700	0.8	15.3	28.1	1.794
3	500	0.4	24.0	28.0	7.703
4	500	0.4	6.5	35.1	7.360
5	700	0.8	15.3	21.2	1.703
6	500	1.2	24.0	27.9	0.895
7	900	1.2	6.5	27.9	0.226
8	900	1.2	24.0	20.9	0.161
9	500	0.4	6.5	35.0	8.664

Table 7. Results for central composite design matrix (Continued)

Run	A: Temperature modification (°C)	B: Steel slag dosage (g/L)	C: Contacting time (h)	Output ammonia concentration (mg NH_3–N/L)	Output phosphate concentration (mg PO_4^{3-}/L)
10	900	0.4	6.5	27.9	3.959
11	700	0.8	15.3	20.8	2.023
12	700	0.8	15.3	21.1	1.915
13	900	0.4	6.5	28.0	3.419
14	900	1.2	24.0	27.8	0.155
15	900	0.4	24.0	28.1	0.422
16	700	0.8	30.0	21.1	1.896
17	700	0.8	0.5	21.2	7.357
18	1036	0.8	15.3	21.1	0.647
19	700	0.1	15.3	28.0	8.606
20	700	0.8	15.3	21.0	1.694
21	500	0.4	24.0	27.8	7.577
22	900	1.2	6.5	28.1	0.221
23	900	1.2	6.5	28.1	0.22
24	900	0.4	24.0	21.2	3.325
25	500	1.2	6.5	28.2	2.083
26	700	1.5	15.3	21.2	2.033
27	700	1.5	15.3	21.0	0.616
28	700	0.8	15.3	20.8	0.654
29	1036	0.8	15.3	21.1	0.824
30	364	0.8	15.3	27.9	6.354
31	700	0.1	15.3	28.2	8.886
32	900	1.2	24.0	28.2	0.245
33	700	0.8	30.0	28.2	2.162
34	900	0.4	24.0	27.8	5.802
35	700	0.8	0.5	21.0	6.639
36	500	1.2	24.0	21.2	1.200
37	900	0.4	6.5	28.1	5.101
38	364	0.8	15.3	28.1	5.752
39	500	1.2	6.5	28.0	1.990
40	700	1.5	15.3	27.8	0.870
41	700	0.8	30.0	28.0	2.392
42	500	0.4	6.5	34.9	8.359
43	500	1.2	6.5	27.8	2.005
44	700	0.1	15.3	27.8	8.976
45	700	0.8	0.5	20.8	7.634
46	500	0.4	24.0	21.2	7.969
47	500	1.2	24.0	28.1	1.444
48	364	0.8	15.3	28.0	5.062

3.3.2 Response as output phosphate concentration

Figure 7a shows the normal probability plot of residuals. As the plot of the residuals approximately followed a straight line, the residuals were normally distributed. Figure 7b demonstrates the relationship between residuals and predicted values of the response. As the points fell randomly on both sides of 0, without recognizable patterns in the points, the residuals were normally distributed with a relatively constant variance. Hence, the regression model met the assumption of normality and homogeneity of variance. Figure 7c illustrates the relation between the response predicted from the empirical model and the actual values obtained from the experiments. Clearly, most data points on the plot were close to the experimental values, as also shown by the high R^2 values (R^2 = 0.906, adjusted R^2 = 0.884, and predicted R^2 = 0.849). The suggested model type for the response was quadratic.

From the ANOVA result in Table 8a, the quadratic model of phosphate concentration was statistically significant ($p<0.0001$). It is obvious that the effects of modified temperature (A), steel slag dosage (B), contact time (C), linear interaction of modified temperature - dosage (AB), second-order effects of dosage (B^2) and reaction time (C^2) were statistically significant while AC and BC interactions and A^2 were insignificant. According to the regression equation in Table 8b, the effects of three main factors on output phosphate concentration were negative, while the AB interaction was positive. The dosage of steel slag had the greatest effect on output phosphate concentration, as evidenced by the coefficient estimate of -2.5. The effect of calcination temperature on phosphate output concentration in this study is consistent with that of Yu et al. (2015), in which the modified steel slag at 800°C provided a higher removal efficiency than the raw material. Similarly, Wang et al. (2021) also stated that the modified granular steel slag at 800°C for 1 h was easier to hydrolyze Ca^{2+}, which

possibly promoted the precipitation of phosphates. In comparison to Wang et al. (2018), the opposite trends were found since the steel slag dosage provided a negative effect on phosphorus removal efficiency, and the effect of reaction time in his study was insignificant. The reason might come from the differences in the selected ranges of the steel slags and contact time from the two studies as we conducted the experiments in a wider range of time (0.5–30 h) but at a lower range of steel slag dosages (0.13–1.47 g/L).

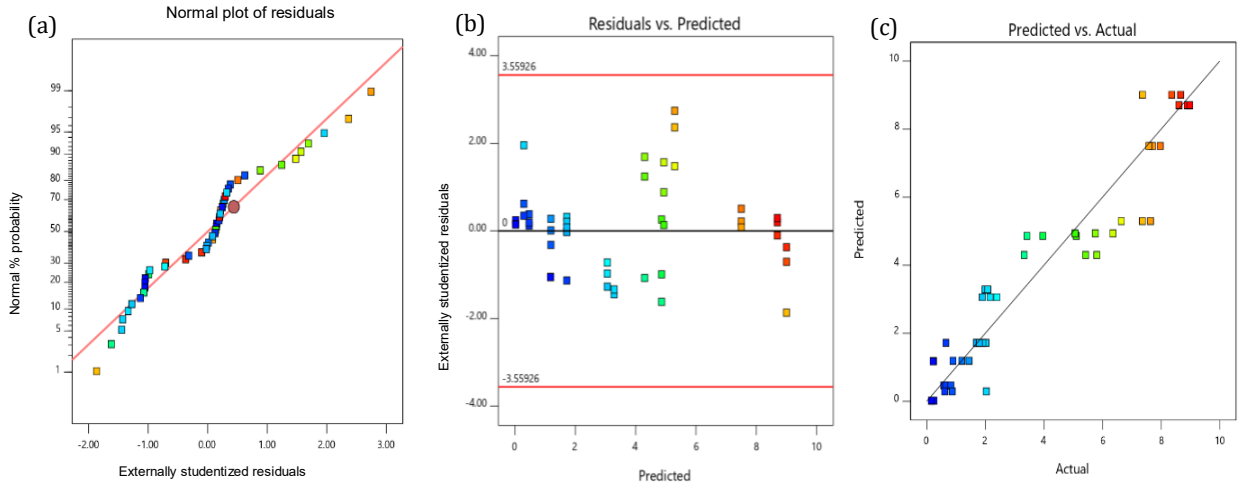

Figure 7. (a) A normal plot of residuals for output phosphate concentration, (b) a plot of residuals versus fitted values for phosphate concentration, and (c) the correlation between the experimental and predicted values of output phosphate concentration

Table 8. ANOVA results for a quadratic model of phosphate concentration and the regression equation of fitted model of the phosphate concentration in coded units

Source	Sum of squares	df	Mean square	F-value	p-value
Model	389.81	9	43.31	40.63	< 0.0001
A-Temperature modification	72.27	1	72.27	67.79	**< 0.0001**
B-Steel slag dosage	255.98	1	255.98	240.13	**< 0.0001**
C-Contacting time	18.11	1	18.11	16.99	**0.0002**
AB	6.22	1	6.22	5.83	**0.0207**
AC	1.32	1	1.32	1.24	0.2721
BC	0.5343	1	0.5343	0.5012	0.4833
A^2	3.37	1	3.37	3.17	0.0832
B^2	26.84	1	26.84	25.18	**< 0.0001**
C^2	21.06	1	21.06	19.75	**< 0.0001**
Residual	40.51	38	1.07		
Lack of Fit	30.34	5	6.07	19.7	< 0.0001
Pure Error	10.16	33	0.308		
Cor Total	430.32	47			

Regression equation: $Y = +1.72 - 1.33A - 2.50B - 0.6648C + 0.5090AB + 0.2349AC - 0.1492BC + 0.3484A^2 + 0.9826B^2 - 0.8703C^2$

3.3.3 Response as ammonia output concentration

Figure 8a shows the normal probability plot of residuals. Similar to the case of phosphate, the plot of the residuals approximately followed a straight line, suggesting that the residuals were normally distributed. The relationship between residuals and predicted values of response (Figure 8b) indicated that the points were distributed randomly on either side of 0 with no discernible patterns. The assumption of normality and homogeneity of variance was therefore satisfied by the regression model. Figure 8c provides the relation between the response predicted from the empirical model and the actual values obtained from the experiments. Clearly, data points on the plot were not that close to the experimental values, which was consistent with the results of the low R^2 values (R^2 = 0.402, adjusted R^2 = 0.2606, and predicted R^2 = 0.0419)

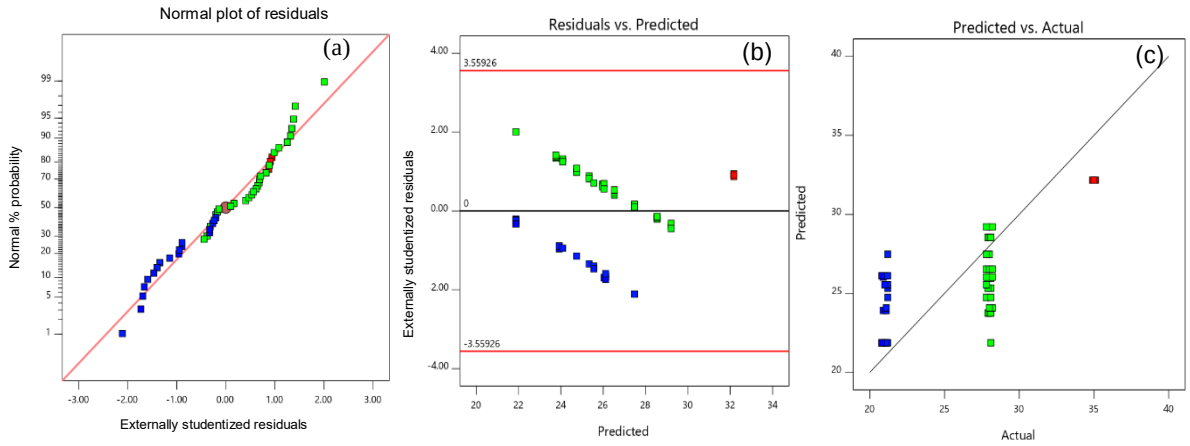

Figure 8. (a) A normal plot of residuals for output ammonia concentration, (b) a plot of residuals versus fitted values for ammonia concentration, and (c) correlation between the experimental and predicted value of output ammonia concentration

Based on the ANOVA result in Table 9, the p-value of 0.0116 implies that the quadratic model of ammonia concentration was significant and there was only a 0.0116% chance that an F-value this large could occur due to noise. In addition, the linear effects of modified temperature (A), quadratic effects of modified temperature (A^2), and steel slag dosage (B^2) were significant model terms while other terms could be neglected. Similar to the result from phosphate treatment, the calcination temperature negatively affected the ammonia output concentration (Table 9), which would be due to the modified steel slag being easier to hydrolyze Ca^{2+}, leading to the promotion of the ion exchange process with Ca^{2+} as a main mechanism of ammonia removal (Wang et al., 2021)

Table 9. ANOVA results for a quadratic model of ammonia concentration and the regression equation of fitted model of the ammonia concentration in coded units

Source	Sum of squares	df	Mean square	F-value	p-value
Model	318.40	9	35.38	2.84	0.0116
A-Temperature modification	77.51	1	77.51	6.22	***0.0171***
B- Steel slag dosage	48.43	1	48.43	3.89	0.0559
C-Contacting time	14.95	1	14.95	1.20	0.2802
AB	17.68	1	17.68	1.42	0.2408
AC	18.03	1	18.03	1.45	0.2364
BC	18.37	1	18.37	1.48	0.2320
A^2	66.03	1	66.03	5.30	***0.0269***
B^2	105.45	1	105.45	8.47	***0.0060***
C^2	36.16	1	36.16	2.90	0.0966
Residual	473.27	38	12.45		
Lack of Fit	243.01	5	48.60	6.97	0.0002
Pure Error	230.25	33	6.98		
Cor Total	791.67	47			

Regression equation: $Y = +21.87 - 1.38A - 1.09B - 0.6040C + 0.8583AB + 0.8667AC + 0.8750BC + 1.54A^2 + 1.95B^2 + 1.14C^2$

3.3.4 Optimization results

3.3.4.1 Optimization for each response

The results of the above sections suggested that the calcination temperature negatively affected both the output phosphate and ammonia concentrations, while the steel slag dosage and the reaction time only impacted the phosphate concentration. This result confirmed the preliminary findings from Section 3.2 in which the changes in output phosphate concentrations from 2 to 24 h of treatment were obvious, but this was not visible for the case of the output ammonia. Figures 9a and 9b show the interaction effect between the temperature and steel slag dosage on both responses. Obviously, favorable conditions for reducing the output phosphate concentration were determined at the top-right corner positions of the plot (Figure 9a). The optimal conditions for minimizing the output ammonia concentration were quite similar to that of phosphate but the areas for selection were broader (Figure 9b).

The optimization for phosphate and ammonia concentrations was first run separately in which the factors were within their ranges, and the response of either phosphate or ammonia was set at "minimum". Tables S1 and S2 in Supplementary Data indicate the strains for each response and the corresponding solutions suggested

by the software, while Figures 9c and 9d illustrate the dependence of desirability on the modified temperature and steel slag dosages for each response. Herein, 100 solutions were suggested for minimizing phosphate effluent concentration with the temperature ranging from 500 to 900°C, contact time from 6.5 to 24 h, and steel slag dosages from 0.6 to 1.2 g/L, by which the expected phosphate output concentration would be from 0 to 1.9 mg/L. There was one solution suggested for minimizing the ammonia effluent concentration at 776°C, 0.872 g/L of modified steel slag, and a contact time of 15.8 h, by which an output concentration of ammonia of 21.5 mg/L would be achieved.

3.3.4.2 Optimum conditions for both responses and experimental validation

To minimize both phosphate and ammonia output concentrations, the optimization conditions for these two responses were considered simultaneously. The three factors were considered in their ranges while both output phosphate and ammonia concentrations were set at minimum values (Table 10a). As can be seen from Table 10b, there were two solutions suggested in which the working conditions, the expected responses from these solutions, and their desirability were close to each other.

Under the modified temperature of 776°C, the dosage of 0.87 g/L, and the contacting time of 15.7 h, the output concentrations of phosphate and ammonia were expected to be 0.84 mg/L (removal efficiency of 91.6%) and 21.5 mg/L (removal efficiency of 48.8%), respectively. This optimal condition was then validated using domestic wastewater. As given in Figure 10, the removal efficiencies of phosphate, ammonia, and COD were 81.7±2.7%, 31.6±20.1%, and 32.7±5.5%, respectively. The removal efficiency achieved from real domestic wastewater was lower than the expected values because the real domestic wastewater contained other contaminants such as COD, color, NO_2^-, NO_3^-, and TSS which possibly competed with ammonia and phosphate for active sites on the surface of the modified steel slags. The removal efficiency of COD mentioned above was evidence for this suggestion. The phosphorus removal efficiency of this study was close to the phosphate removal efficiencies found by Wang et al. (2021) and Pramanik et al. (2020) who also treated domestic and municipal wastewater with steel slags and achieved removal efficiencies of 82.5% and 82%, respectively. However, the efficiency in this study was lower than that of J.-H. Park et al. (2017) at 89.3%, and Ping et al. (2016) at 99%. This is possibly due to the differences in wastewater characteristics, as J.-H. Park et al. (2017) used wastewater discharged from hydroponic cultivation and Ping et al. (2016) treated synthetic wastewater. The ammonia treatment efficiency achieved by this study was also higher than those of Ping et al. (2016) and Wang et al. (2021) who found ammonia removal efficiencies of 22.3% and 15%, respectively, from domestic wastewater.

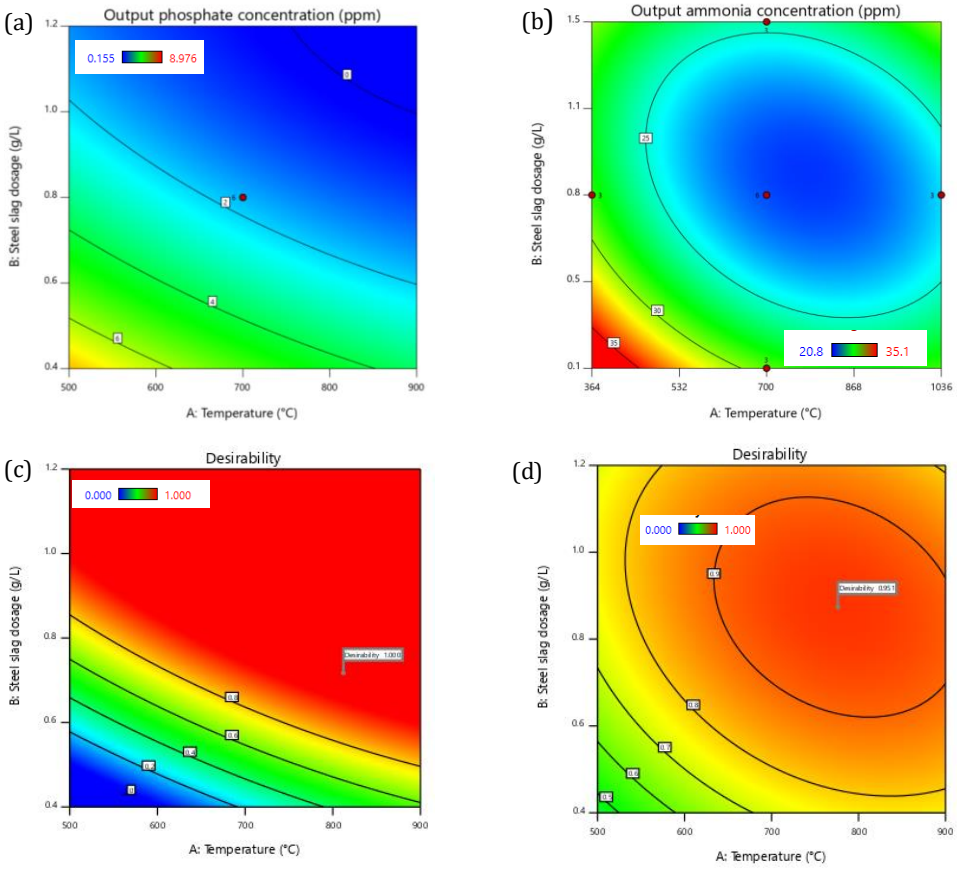

Figure 9. Contour plots (2D) with factors' interaction for the response: (a) phosphate and (b) ammonia output concentrations; and desirability according to calcination temperature and steel slag dosages for (c) phosphate and (d) ammonia output concentrations

Table 10. (a) Constraints for optimization of both phosphate and ammonia output concentrations and (b) The suggested solutions

(a)

Name	Goal	Lower limit	Upper limit
A: Temperature	is in range	500	900
B: Steel slag dosage	is in range	0.4	1.2
C: Contacting time	is in range	6.5	24
Output ammonia conc.	minimize	21	35
Output phosphate conc.	minimize	2	6

(b)

Number	Temperature (°C)	Steel slag dosage (g/L)	Contacting time (h)	Output ammonia concentration (mg NH_3-N/L)	Output phosphate concentration (mg PO_4^{3-}P/L)	Desirability
1	776	0.87	15.7	21.5	0.844	0.975
2	777	0.88	15.6	21.5	0.833	0.975

Though the output phosphorus concentration was 1.5 mg/L which is an allowable value from Column A of QCVN 14:2008/BTNMT (6 mg/L), the output ammonia concentration (16.33 mg/L) was higher than the recommended value (5 mg/L). Hence, further investigation for enhancing the treatment of ammonia is necessary. In addition, this study did not conduct tests to create the breakthrough curves for the estimation of the possible working time of the material, and the way to recover the material after adsorption saturation. Such tests are important in the future to increase the feasibility of the real application of steel slags.

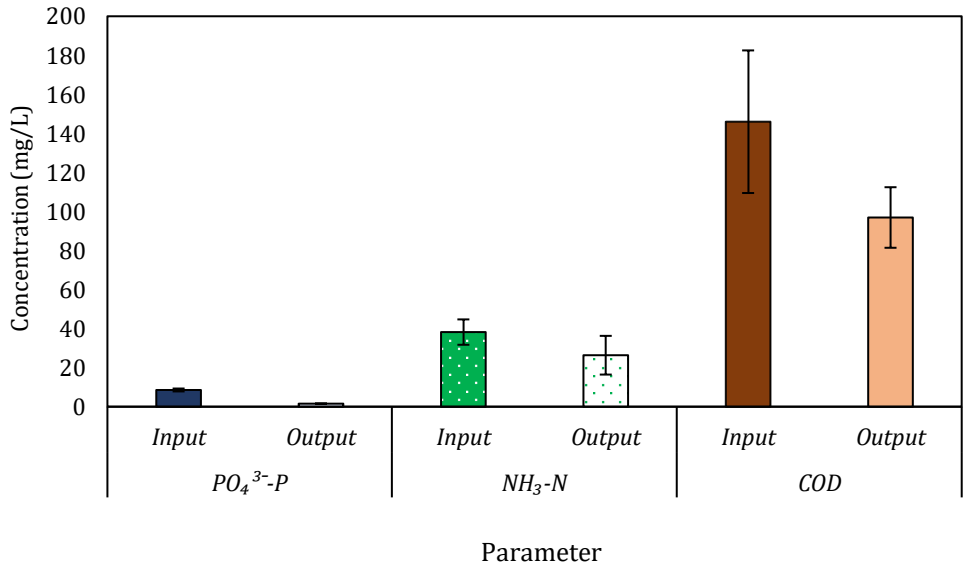

Figure 10. The concentration of parameters in domestic wastewater before and after the treatment by modified steel slag adsorbent at optimum conditions

4. CONCLUSION

This study investigated the application of steel slags and their thermally modified material for the adsorption of phosphate and ammonia in domestic wastewater. Steel slags were collected, thermally modified, and characterized via SEM, EDS, and BET. The results showed that the increase of heating temperature from 0 to 900°C led to significant reductions of the mass percentages, from 10.03% to 3.98% for C elements and from 53.13 to 37.06% for O elements, while Ca elements increased from 34.48 to 55.5%. Also, the increase in calcination temperature resulted in an increase in the surface area of the material. After selecting the type of steel slag from the preliminary test, their adsorption kinetics and isotherms were studied. RSM using CCD was then applied for the adsorption optimization process with three factors (modified temperature, adsorbent dosage, and reaction time) and two responses (output concentrations of phosphate and ammonia). The results indicated that the modified temperature, adsorbent dosage, and reaction time significantly affected output phosphate concentration,

while the output ammonia concentration was influenced by modified temperature and adsorbent dosage. Optimal conditions were identified at a modified temperature of 776°C, an adsorbent dosage of 0.87 g/L, and a contact time of 15.7 h by which the removal efficiencies achieved 81.7% for phosphate, 31.6% for ammonia, and 32.7% for COD from domestic wastewater. Though phosphate output concentration (1.4 mg/L) was within the allowable value, ammonia and COD required further treatments.

ACKNOWLEDGMENT

This research is funded by Vietnam National University HoChiMinh City (VNU-HCM) under grant number C2022-28-07. We would also like to thank the Da Nang Steel Joint Stock Company (DN), and Green Materials Co., Ltd from Ba Ria–Vung Tau (GM) for their support in the steel slags collection.

REFERENCES

Abd El-Azim, H., El-Sayed Seleman, M. M., and Saad, E. M. (2019). Applicability of water-spray electric arc furnace steel slag for removal of Cd and Mn ions from aqueous solutions and industrial wastewaters. *Journal of Environmental Chemical Engineering,* 7(2), 102915.

Ahmad, S. Z. N., Hamdan, R., Al-Gheethi, A., Alkhadher, S., and Othman, N. (2020). Removal of phosphate from wastewater by steel slag with high calcium oxide column filter system; efficiencies and mechanisms study. *Journal of Chemical Technology and Biotechnology,* 95(12), 3232–3240.

Ambulkar, A. R. (2017). *Nutrient Pollution and Wastewater Treatment Systems.* Oxford Research Encyclopedia of Environmental Science.

APHA, AWWA, and WEF. (2005). *Standard Methods for the Examination of Water and Wastewater*, 21st, Washington, DC: American Public Health Association.

Barca, C., Meyer, D., Liira, M., Drissen, P., Comeau, Y., Andrès, Y., and Chazarenc, F. (2014). Steel slag filters to upgrade phosphorus removal in small wastewater treatment plants: Removal mechanisms and performance. *Ecological Engineering,* 68, 214–222.

Bowden, L. I., Jarvis, A. P., Younger, P. L., and Johnson, K. L. (2009). Phosphorus removal from waste waters using basic oxygen steel slag. *Environmental Science & Technology,* 43(7), 2476–2481.

da Silva, J. M., da Silva, C. E. P., Freire, J. M. A., Becker, H., Diógenes, I. C. N., and Longhinotti, E. (2022). Industrial steel waste-based adsorbent: An effective phosphate removal from aqueous media. *Materials Chemistry and Physics,* 292, 126828.

Dhoble, Y., and Ahmed, S. (2018). Column studies for the simultaneous removal of phenol, ammonia and thiocyanate by the adsorption with steel slag. *International Journal for Research in Applied Science and Engineering Technology*, 6(1), 2919–2929.

Dunets, C. S., and Zheng, Y. (2014). Removal of phosphate from greenhouse wastewater using hydrated lime. *Environmental Technology,* 35(21-24), 2852–2862.

Fang, D., Huang, L., Fang, Z., Zhang, Q., Shen, Q., Li, Y., Xu, X., and Ji, F. (2018). Evaluation of porous calcium silicate hydrate derived from carbide slag for removing phosphate from wastewater. *Chemical Engineering Journal*, 354, 1–11.

Gao, H., Song, Z., Zhang, W., Yang, X., Wang, X., and Wang, D. (2017). Synthesis of highly effective absorbents with waste quenching blast furnace slag to remove methyl orange from aqueous solution. *Journal of Environmental Sciences*, 53, 68–77.

Garrido-Cardenas, J. A., Esteban-García, B., Agüera, A., Sánchez-Pérez, J. A., and Manzano-Agugliaro, F. (2020). Wastewater treatment by advanced oxidation process and their worldwide research trends. *International Journal of Environmental Research and Public Health,* 17(1), 170.

Gwon, H. S., Khan, M. I., Alam, M. A., Das, S., and Kim, P. J. (2018). Environmental risk assessment of steel-making slags and the potential use of LD slag in mitigating methane emissions and the grain arsenic level in rice (*Oryza sativa* L.). *Journal of Hazardous Materials,* 353, 236–243.

Hamdan, R., Ibrahim, I. I., Wan Mohamed, W. A., Al-Gheethi, A., Othman, N., and Mohamed, R. (2021). Optimizing vertical flow aerated steel slag filter system with nitrifiers bacteria for nutrients' removal from domestic wastewater: A pilot study. *Journal of Chemical Technology and Biotechnology,* 96(4), 1067–1079.

Han, C., Wang, Z., Yang, H., and Xue, X. (2015). Removal kinetics of phosphorus from synthetic wastewater using basic oxygen furnace slag. *Journal of Environmental Sciences,* 30, 21–29.

Hua, G., Salo, M. W., Schmit, C. G., and Hay, C. H. (2016). Nitrate and phosphate removal from agricultural subsurface drainage using laboratory woodchip bioreactors and recycled steel byproduct filters. *Water Research,* 102, 180–189.

Jafari, J. A., and Moslemzadeh, M. (2022). Investigation of phosphorus removal using steel slag from aqueous solutions: A systematic review study. *International Journal of Environmental Analytical Chemistry,* 102(4), 821–833.

Jha, V. K., Kameshima, Y., Nakajima, A., and Okada, K. (2008). Utilization of steel-making slag for the uptake of ammonium and phosphate ions from aqueous solution. *Journal of Hazardous Materials,* 156(1–3), 156–162.

Ji, R., Liu, T.-J., Kang, L.-L., Wang, Y.-T., Li, J.-G., Wang, F.-P., Yu, Q., Wang, X.-M., Liu, H., Guo, H.-W., Xu, W.-L., Zeng, Y.-N., and Fang, Z. (2022). A review of metallurgical slag for efficient wastewater treatment: Pretreatment, performance and mechanism. *Journal of Cleaner Production,* 380(2), 135076.

Jinming, D., Jinmei, L., Hangda, F., Jianqing, L., and Sanmei, L. (2012). Adsorption characteristic of modified steel-making slag for simultaneous removal of phosphorus and ammonium nitrogen from aqueous solution. *Chinese Journal of Environmental Engineering,* 6(1), 201–205.

Kadirova, Z. C., Hojamberdiev, M., Bo, L., Hojiyev, R., and Okada, K. (2015). Simultaneous removal of NH_4^+, $H_2PO_4^-$ and Ni^{2+} from aqueous solution by thermally activated combinations of steel converter slag and spent alumina catalyst. *Journal of Water Process Engineering, 8*, 151–159.

Kermani, M., Bina, B., Movahedian, H., Amin, M. M., and Nikaeen, M. (2009). Biological phosphorus and nitrogen removal from wastewater using moving bed

biofilm process. *Iranian Journal of Biotechnology,* 7(1), 19–27.

Kilpimaa, S., Runtti, H., Kangas, T., Lassi, U., and Kuokkanen, T. (2015). Physical activation of carbon residue from biomass gasification: novel sorbent for the removal of phosphates and nitrates from aqueous solution. *Journal of Industrial Engineering Chemistry,* 21, 1354–1364.

Kim, E.-H., Lee, D.-W., Hwang, H.-K., and Yim, S. (2006). Recovery of phosphates from wastewater using converter slag: Kinetics analysis of a completely mixed phosphorus crystallization process. *Chemosphere,* 63(2), 192–201.

Li, J., Wu, B., Zhou, T., and Chai, X. (2018). Preferential removal of phosphorus using modified steel slag and cement combination for its implications in engineering applications. *Environmental Technology & Innovation,* 10, 264–274.

Lim, L. H., Regina, L. Z. L., Soh, Y. T., and Teo, S. S. (2018). Determination of levels of phosphate, ammonia and chlorine from indoor and outdoor nano tank system. *International Journal of Aquaculture,* 8(19), 145–150.

Liu, M., Liu, X., Wang, W., and Guo, J. (2022). Phosphorus removal from wastewater using electric arc furnace slag aggregate. *Environmental Technology,* 43(1), 34–41.

Luo, W., Phan, H. V., Xie, M., Hai, F. I., Price, W. E., Elimelech, M., and Nghiem, L. D. (2017). Osmotic versus conventional membrane bioreactors integrated with reverse osmosis for water reuse: Biological stability, membrane fouling, and contaminant removal. *Water Research,* 109, 122–134.

Mahmoodi, N. M., and Maghsoodi, A. (2015). Kinetics and isotherm of cationic dye removal from multicomponent system using the synthesized silica nanoparticle. *Desalination and Water Treatment,* 54(2), 562–571.

Mockler, E. M., Deakin, J., Archbold, M., Gill, L., Daly, D., and Bruen, M. (2017). Sources of nitrogen and phosphorus emissions to Irish rivers and coastal waters: Estimates from a nutrient load apportionment framework. *Science of the Total Environment*, 601–602, 326–339.

Mokhtari-Shourijeh, Z., Langari, S., Montazerghaem, L., and Mahmoodi, N. M. (2020). Synthesis of porous aminated PAN/PVDF composite nanofibers by electrospinning: Characterization and Direct Red 23 removal. *Journal of Environmental Chemical Engineering,* 8(4), 103876.

MONRE. (2008). *QCVN 14: 2008/BTNMT: National technical regulation on domestic wastewater* (Decision No. 16/2008/QD-BTNMT dated December 31, 2008). Minister of Natural Resources and Environment.

Oguz, E. (2004). Removal of phosphate from aqueous solution with blast furnace slag. *Journal of Hazardous Materials,* 114(1), 131–137.

Park, J.-H., Wang, J. J., Kim, S.-H., Cho, J.-S., Kang, S.-W., Delaune, R. D., and Seo, D.-C. (2017). Phosphate removal in constructed wetland with rapid cooled basic oxygen furnace slag. *Chemical Engineering Journal,* 327, 713–724.

Park, T., Ampunan, V., Maeng, S., and Chung, E. (2017). Application of steel slag coated with sodium hydroxide to enhance precipitation-coagulation for phosphorus removal. *Chemosphere,* 167, 91–97.

Ping, X., Liyun, Y., Aikebaier, R., and Hao, B. (2016). The removal of phosphate and ammonia nitrogen from wastewater using steel slag. In *Energy Technology 2015 Carbon Dioxide Management and Other Technologies* (Jha, A., Wang, C., Neelameggham, N. R., Guillen, D. P., Li, L., Belt, C. K., Kirchain, R., Spangenberger, J. S., Johnson, F., Gomes, A. J., Pandey, A., and Hosemann P., Eds.), pp. 165–172. Cham: Springer.

Pramanik, B. K., Islam, M. A., Asif, M. B., Roychand, R., Pramanik, S. K., Shah, K., Bhuiyan, M., and Hai, F. (2020). Emerging investigator series: phosphorus recovery from municipal wastewater by adsorption on steelmaking slag preceding forward osmosis: An integrated process. *Environmental Science: Water Research & Technology,* 6(6), 1559–1567.

Preisner, M., Neverova-Dziopak, E., and Kowalewski, Z. (2020). Analysis of eutrophication potential of municipal wastewater. *Water Science and Technology,* 81(9), 1994–2003.

Qiu, Q., Gao, M., Zhou, W., Xu, Z., Kong, C., Qiu, L., Zhang, S., and Sun, S. (2022). Enhanced phosphorus removal during municipal wastewater treatment by the biological aeration filter with modified steel slags. *Journal of Environmental Engineering,* 148(5), 04022016.

Qiu, R., Cheng, F., Wang, X., Li, J., and Gao, R. (2015). Adsorption kinetics and isotherms of ammonia-nitrogen on steel slag. *Desalination and Water Treatment,* 55(1), 142–150.

Roychand, R., Pramanik, B. K., Zhang, G., and Setunge, S. (2020). Recycling steel slag from municipal wastewater treatment plants into concrete applications – a step towards circular economy. *Resources, Conservation and Recycling*, 152, 104533.

Sahoo, T. R., and Prelot, B. (2020). Adsorption processes for the removal of contaminants from wastewater: The perspective role of nanomaterials and nanotechnology. In *Nanomaterials for the Detection and Removal of Wastewater Pollutants* (Bonelli, B., Freyria, F. S., Rossetti, I., and Sethi R., Eds.), pp. 161–222, Amsterdam: Elsevier.

Shi, C., Wang, X., Zhou, S., Zuo, X., and Wang, C. (2022). Mechanism, application, influencing factors and environmental benefit assessment of steel slag in removing pollutants from water: A review. *Journal of Water Process Engineering,* 47, 102666.

Sibiya, N. P., Amo-Duodu, G., Kweinor Tetteh, E., and Rathilal, S. (2022). Response surface optimisation of a magnetic coagulation process for wastewater treatment via Box-Behnken. *Materials Today: Proceedings,* 62, S122–S126.

Song, X., Pan, Y., Wu, Q., Cheng, Z., and Ma, W. (2011). Phosphate removal from aqueous solutions by adsorption using ferric sludge. *Desalination,* 280(1–3), 384–390.

Steinman, A. D., Hassett, M., Oudsema, M., and Penn, C. J. (2022). Reduction of phosphorus using electric arc furnace slag filters in the Macatawa watershed (Michigan). *Frontiers in Environmental Science,* 10, 863137.

Trang, T. T. T., Long, H. T., Dung, P. T., Tung, H. V., Sang, N. X., and Nuong, N. T. (2018). A study of microstructure of steel slags used for pollutants adsorption and removal in waste water. *VNU Journal of Science: Earth and Environmental Sciences,* 34(4), 1–9.

Trinh, V. M, Minh, N. T., Thao, N. T. P., Phuong, P. L., and Tuyen, T. V. (2023). Study on recycle of granulated blast-furnace slag as an adsorbent for ammonium remediation in wastewater. *Vietnam Journal of Science and Technology,* 61(4), 609–619.

Trinh, V. T., Do, V. M., Nguyen, T. M., Pham, T. D., Van, H., and Trinh, V. M. (2022). Study on the recycle of steel slag as

an adsorbent for COD removal in pulp mill wastewater. *Vietnam Journal of Science and Technology,* 60(4), 675–690.

Wang, J., Wang, X., Qiu, L., Li, T., and Yu, C. (2018). Study on key factors of adsorption of phosphorus by steel slag filter based on response surface method. *E3S Web of Conferences*, 53, 03050.

Wang, S., Yao, S., Du, K., Yuan, R., Chen, H., Wang, F., and Zhou, B. (2021). The mechanisms of conventional pollutants adsorption by modified granular steel slag. *Environmental Engineering Research,* 26(1), 190352.

Xue, Y., Hou, H., and Zhu, S. (2009). Characteristics and mechanisms of phosphate adsorption onto basic oxygen furnace slag. *Journal of Hazardous Materials,* 162(2–3), 973–980.

Yan, Y., Sun, X., Ma, F., Li, J., Shen, J., Han, W., Liu, X., and Wang, L. (2014). Removal of phosphate from wastewater using alkaline residue. *Journal of Environmental Sciences,* 26(5), 970–980.

Yang, L., Yang, M., Xu, P., Zhao, X., Bai, H., and Li, H. (2017). Characteristics of nitrate removal from aqueous solution by modified steel slag. *Water,* 9(10), 757.

Yu, J., Liang, W., Wang, L., Li, F., Zou, Y., and Wang, H. (2015). Phosphate removal from domestic wastewater using thermally modified steel slag. *Journal of Environmental Sciences,* 31, 81–88.

Zhao, Y., Tong, X., and Chen, Y. (2021). Fit-for-purpose design of nanofiltration membranes for simultaneous nutrient recovery and micropollutant removal. *Environmental Science & Technology,* 55(5), 3352–3361.